A Density Functional Theory Study of Adsorption Ethionamide on the Surface of the Pristine, Si and Ga and Al-Doped Graphene

Vessally, Esmail*+; Musavi, Mahla; Poor Heravi, Mohammad Reza
Department of Chemistry, Payame Noor University, Tehran, I.R. IRAN

Hosseinian, Akram
School of Engineering Science, College of Engineering, University of Tehran, Tehran, I.R. IRAN

ABSTRACT: *In this research, the adsorption behavior of pristine, Si- and Ga- and Al-doped graphene is investigated toward ethionamide (EA) using Density Functional Theory (DFT) calculations. Total energies, and geometry optimizations were obtained and Density of State (DOS) analysis was performed at B3lyp level of theory with the 6-31G* basis set. The adsorption energy (E_{ad}) between EA and the pristine, Si-, Ga- and Al-doped graphene is changed in the following order: Ga-Complex-N(ring) > Al- Complex-N(ring) > Si-Complex-N(ring) > Complex-S. The E_{ad} of the Graphene-EA complex is -2.552 kcal/mol, which is low and shows that the adsorption is physical. The % ΔE_g = -59.61% for Si-doped graphene EA shows the high sensitivity of the Si-doped graphene to the adsorption of EA. The E_g for Ga-doped graphene-EA decreases significantly from 2.35 to 1.11 eV and the rate of change is %ΔE_g = -52.75%, showing the high sensitivity of Ga-doped graphene to the adsorption of EA. However, the high E_{ad} of -36.66 kcal/mol shows that the Ga-doped graphene can be used as a suitable sensing device only at higher temperatures. The % ΔE_g= -58.98 % for Al-doped graphene-EA indicates the high sensitivity of the Al-doped graphene to the adsorption of EA. The E_{ad} of -34.53 kcal/mol can be used as a suitable sensing device only at higher temperatures.*

KEYWORDS: *Adsorption; Graphene; Etionamide; DFT calculations; Optimization.*

INTRODUCTION

Ethionamide (EA) is a drug used for all cases of pulmonary tuberculosis and extra-pulmonary tuberculosis. EA belongs to a group of drugs called antibiotics. antibiotics are a very important element in modern life and are used to treat diseases. In the last decade, a number of scientists become interested in the environmental effects of drugs that accumulated in the environment in large quantities and their side effects on living organisms are horrible [1].

Aheren et al observed some drugs such as tetracycline and erythromycin remained in the environment [2]. In some studies, more than 60 drugs have been reported

* *To whom correspondence should be addressed.*
+ *E-mail*: *vessally@pnu.ac.ir ; vessally@yahoo.com*
1021-9986/2021/6/1720-1736 12/$/6.02

as the drug contaminants in soil and water of different countries [3, 4]. Types of Drug contamination in the environment, directly and indirectly, affect human, animal, and plants health [5-8].

When a drug is released in large quantities into the environment, it is necessary that it should be identified by a sensor to determine where the drug accumulated. The sensors are needed for the identification of the released drugs and the main group of the sensor can be the nanoparticles [9, 10]. Nanostructures have received much attention as chemical sensors [11-13].

Graphene is synthesized by a variety of techniques, including mechanical exfoliation, chemical synthesis, epitaxial growth on silicon carbide (SiC), Chemical Vapor Deposition (CVD), and other methods. Among these methods, the most popular and promising way to synthesize graphene is CVD because it can produce high-quality graphene on a large scale [14-16]. In graphene, each carbon atom is covalently bonded to three other carbon atoms which achieve great stability and a very high tensile strength. Since graphene is flat, every atom on the surface is accessible from both sides, so there is stronger interaction with surrounding molecules. Also, the carbon atoms are bonded to only three other atoms, although they have the capability to bond to a fourth atom. This capability, combined with the aforementioned tensile strength and high surface area to volume ratio of graphene may make it attractive for use in composite materials. Graphene also has higher electron mobility that is higher than any known material. Modifying the surface structure of the nanosheet by placing impure atoms is a promising way to improve its sensitivity to drug or gas molecules [17].

In a study conducted by *Ghiasi, et al*, the separation of CH_4, H_2S, N_2, and CO_2 gases has been done using four types of nanoporous graphene clusters based on the quantum chemical investigation. The results of this study suggest using a porous graphene sheet as a highly efficient and highly selective membrane for gas separations [18].

In a study conducted by *Mohammad Hussein et al*, the electronic and adsorption properties of the graphene interacted with 5-fluorouracil molecule (5-FU) were theoretically investigated in the gas phase using the B3LYP method. They found that the adsorption behavior of the (5-FU) molecule on the graphene is electrostatic in nature [19]. In another study by *Edjlali et al*, to find a nanosensor to detect sulfanilamide (SA) drug, computationally investigated and interaction with the pristine and Al-doped graphene-like boron nitride nanosheets have studied. The results indicate that the Al-BN may be a promising electronic and type sensor for the SA drug [20]. In recent years, the use of computational chemistry and molecular modeling with the help of computers has attracted the attention of chemists.

In this manuscript, the sensing ability of pristine, Si and Ga, and Al-doped graphenes were studied in identifying the EA drug. The interaction of EA with the pristine graphene and graphene doped with the Al, Ga (from group IIIA), and Si (from group IVA) was investigated to find the preferred adsorption sites, interaction energies, sensing ability using DFT calculations. Also, it has been shown that replacing a carbon atom in graphene with Si, Ga, and Al is a useful way to improve the electronic properties sensing ability. The results of this research can be useful for making an adsorbent for the EA drug and provide suitable sensing.

THEORETICAL SECTION

Methods

In this study, all calculations were performed using the DFT method at the theoretical level of B3LYP / 6-31G* using the Gaussview 05 and GAMESS programs [21]. The B3LYP method is the commonest density functional in the nanostructured-based material study [22-24]. Also, a literature review indicates that the B3LYP is a suitable and reliable density functional for predicting the structural, optic, electronic and energetic properties of different nanostructures [25-31]. The DFT method is one of the most powerful methods in quantum calculations. In the optimization process, the desired molecular structures are optimized to achieve the minimum energy and the energy of the desired systems are calculated [32]. To ensure the lowest energy for the graphene-EA complex rather than a local minimum, the Potential Energy Surface (PES) scans were performed concerning various dihedral angles (D). The Gauss sum was used for drawing the DOS plots [33].

The adsorption energy (E_{ad}) is calculated as follows:

$$E_{ad} = E(drug/adsorbent) - E(adsorbent) - E(drug) + E(BSSE) \quad (1)$$

Where E(adsorbent) is the total energy on an intrinsic or extrinsic molecule.

E(drug/adsorbent) is the total energy of the adsorbed drug molecule on the adsorbent surface.

E(BSSE) is the Basis Set Superposition Error (BSSE) corrected for all adsorption energies using the counterpoise method [34]. In this study, some interaction indicators that are useful for analysis were evaluated.

Theory

A sensor is a device that responds to a specific stimulus and produces a measurable electrical signal. The LUMO - HOMO energy gap (E_g) of the structures under study is computed as follows:

$$Eg = E_{LUMO} - E_{HOMO} \tag{2}$$

The HOMO-LUMO gap is the difference between LUMO and HOMO that showed with Eg [35-54].

When we evaluate the electronic sensitivity of the nanostructure to a drug, the HOMO and LUMO energy deformation are calculated as follows:

$$\%\Delta E_g = \left[\left(E_{g2} - E_{g1} \right) / E_{g1} \right] \times 100 \tag{3}$$

RESULTS AND DISCUSSIONS

In continuation of the previous works on the various fields of organic compounds [55-82], in this work, the adsorption of ethionamide on the surface of the pristine, Si and Ga, and Al-doped graphene was investigated.

The Graphene characterization

The optimized structure of graphene is shown in Fig. 1, where different types of C-C bonds can be identified with equilibrium distances of 1.41, 1.42 A^0. It consists of 57 C and 18 H atoms, and the ends of the atoms are saturated with 18 hydrogen atoms to avoid boundary effects. As shown by DOS plot in (Fig. 1). The HOMO energy of graphene is approximately -4.93 eV and the LUMO energy is -2.10 eV (Table 1), (Fig. 2). Thus, the E_g is approximately 2.82eV (Table 1). Fig. 2 shows that the levels of HOMO and LUMO are mainly located on the C-C atoms, respectively.

The adsorption of EA on the Graphene

Graphene-EA complex

To find a stable structure, it is necessary to perform optimization calculations. In the optimization method, the molecules are optimized using the appropriate method

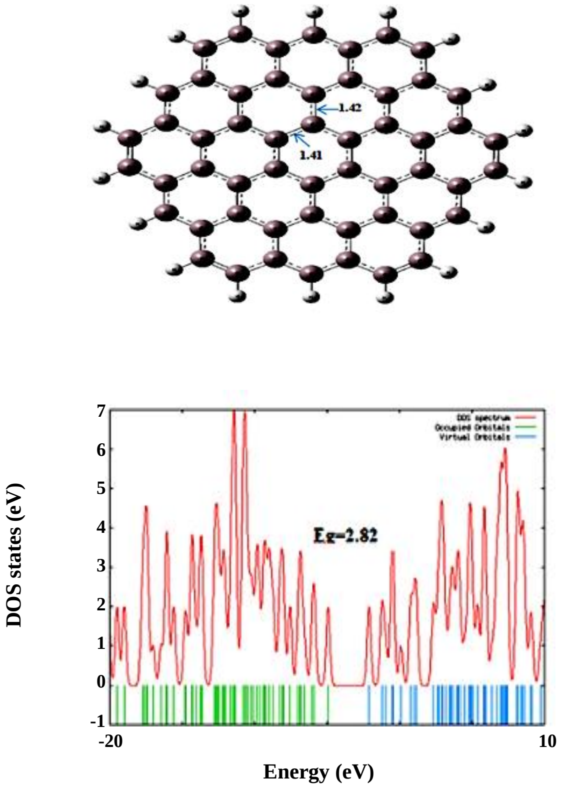

Fig. 1: Optimized structures of graphene and density of state (DOS) plot.

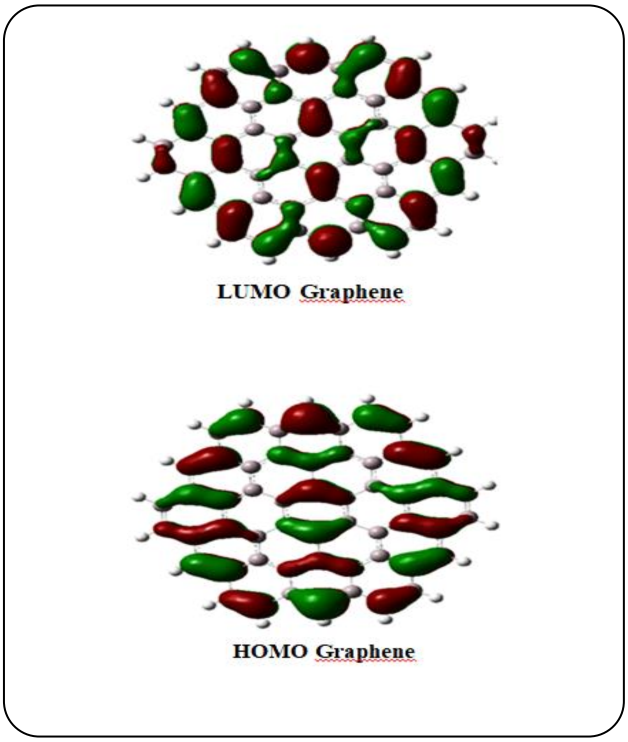

Fig. 2: The HOMO and LUMO profiles of graphene.

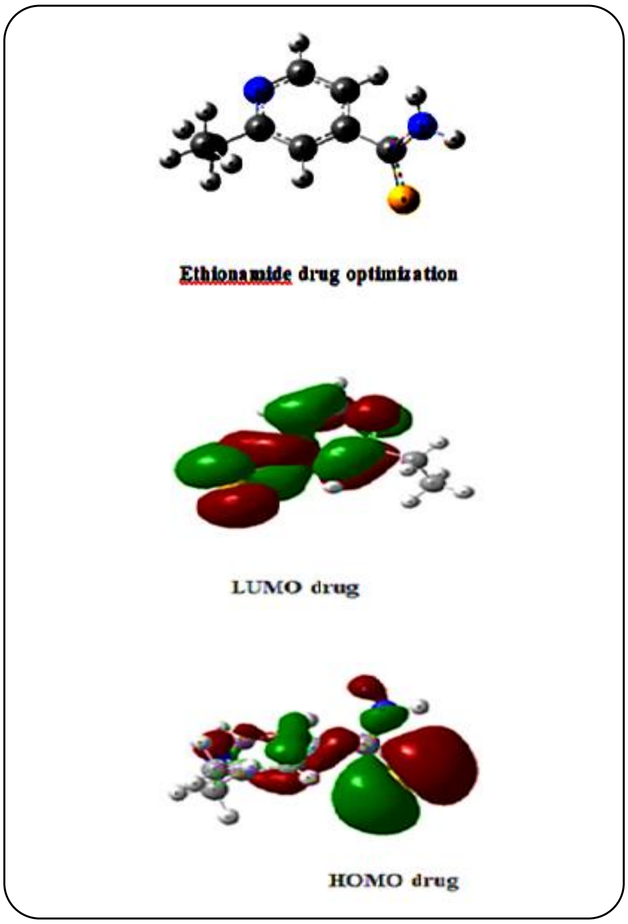

Fig. 3: Optimized structure of EA and its HOMO, and LUMO profiles.

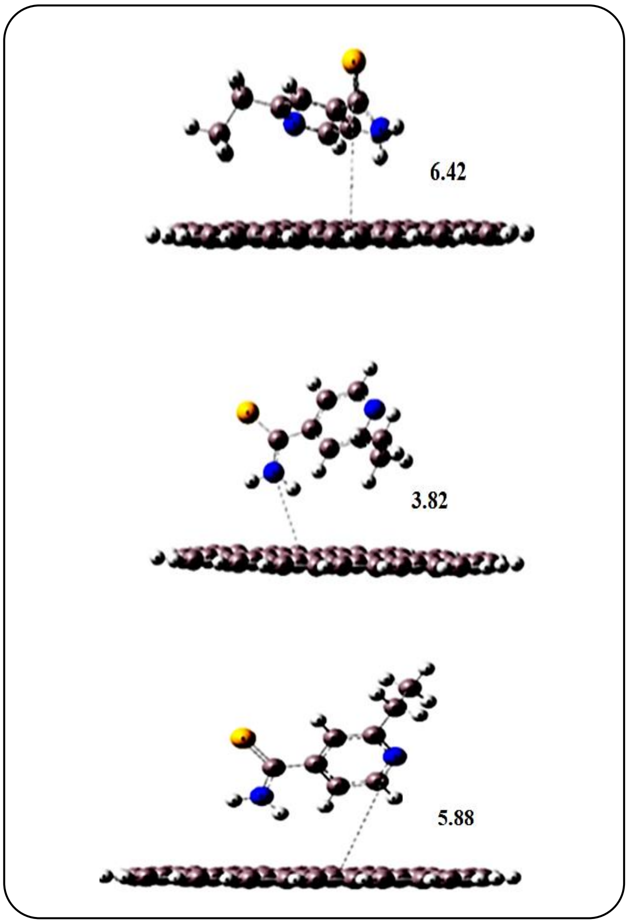

Fig. 4: Optimized structures of graphene-EA complexes. Distances are in Å.

for calculating the interatomic forces, so that the atoms are rearranged to obtain the maximum adsorption energy.

The optimization process is performed to achieve the lower energy structure of ethionamide (EA) (Fig. 3). In order to find the stable configurations (global minima) of an EA drug adsorbed on the graphene, various studies have been carried out. Finally, three active sites of the drug are predicted, including C=S, $-NH_2$ and N(ring), which the drug can adsorb onto the C atom of graphene. As shown in Fig. 4, we obtained three types of complexes that indicate the interactions between C=S, $-NH_2$, N(ring) in EA and the C atom of graphene. The density of state plot (DOS), LUMO, and HOMO have been presented in Fig. 5 for the most stable complexes. It has been found that there are two important parameters including E_{ad} and E_g in the drug sensing potential by nanostructures. In the most stable complex-S, the drug adsorbed from the S atom onto graphene with a distance of 6.42 Å. The adsorption energy is -2.552 kcal/mol which shows a weak interaction and Indicates adsorption in the range of physical adsorption. In Fig. 3, the HOMO of EA is more focused on the S atom and then NH_2 whereas the LUMO has broadly surrounded all three functional groups. The DFT calculations showed that the electronic properties of the graphene have been changed during the absorption of the drug molecule. According to Table 1 and Fig. 5, the HOMO has been changed from -4.93 in the pristine graphene to -5.10 eV in the complex and the LUMO has been changed from -2.10 to -2.30 eV and shifted to lower energy. These changes are to the extent that the LUMO and HOMO are located on the nanostructure atoms. The drug molecule donates a pair of electrons from its nitrogen atoms to the boron atom which has electron deficiency on the graphene surface. As mentioned, two important parameters, i.e., E_{ad} and E_g in the drug sensing potential by nanostructures. The adsorption of EA onto the graphene may be reversible if the E_{ad} is in a suitable range.

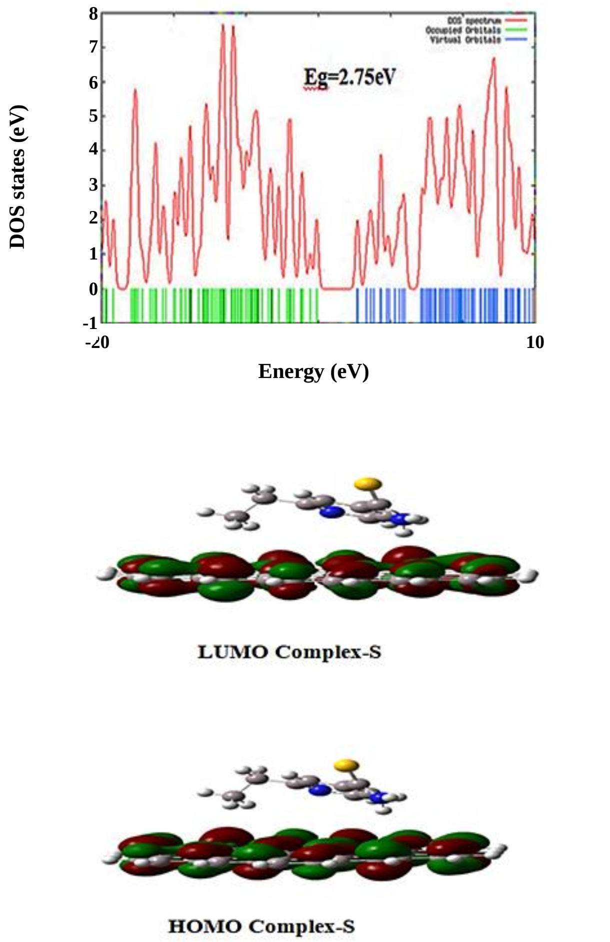

Fig. 5: Density of states (DOS) plot of graphene-EA (Complex-S), and the HOMO, and LUMO profiles of Complex-S.

Strong interactions are not favorable in drug sensing because of a long recovery time and thus hard desorption of a drug over a nanoparticle. With more negative E_{ad}, the recovery time (τ) is increased and this may be determined using the following equation [83, 84].

$$\tau = \nu_0^{-1} \exp\left(-E_{ad}/kT\right) \qquad (4)$$

Here τ is the recovery time and ν_0 is the attempt frequency, T is the temperature, and K is the Boltzmann constant [85].

According to this equation, there is an exponential relationship between E_{ad} and recovery time. The large recovery time is the main problem that can be solved by heating the sensor to a high temperature [86]. Vacuum-UV is applied for the recovery of drugs from the surface of the graphene system.

The second most important factor in sensing character is the energy gap (E_g) of the graphene in the presence of the EA. It has been indicated that the E_g is proportional to the conduction electron population (σ) presented in Eq (5). σ increases when the energy gap (E_g) decreases with adsorption of EA onto the graphene. On the other hand, when the $-\%\Delta E_g$ increases, the potential sensing also increases. The correlation between E_g and the electrical conductance of nanostructures is as follows:

$$\sigma = A T^{3/2} \exp\left(-E_{ad}/2kT\right) \qquad (5)$$

Where k is the Boltzmann's constant, and A (electrons/$m^3K^{3/2}$) is a constant. There is an acceptable correlation between the obtained results of this procedure and experimental techniques [87]. Equation (5) is used to investigate the sensitivity of a nanostructure toward a drug. As a result, electrical conductivity can be converted into an electrical signal related to the presence of drug molecules [88, 89].

The E_g of the graphene decreased when it adsorbed the drug, changing the E_g slightly from 2.82eV to 2.75eV in the complex with $\%\Delta E_g$= -1.02% which shows the low sensitivity of the graphene to the absorption of EA. The change in E_g is not suitable for the sensing ability, the adsorption energy, E_{ad}= -2.552 kcal/mol is so weak that the graphene can not effectively absorb the drug. So, graphene does not a suitable sensing ability with respect to adsorption energy for EA.

In the complex-N(NH_2), EA is adsorbed from the N atom onto the C atom of the graphene at a distance of 3.82Å, and the E_{ad} = -2.522 kcal/mol, which shows that adsorption is weak with ΔE_g = -0.23%.

In a complex-N(ring), EA is adsorbed from the N atom in the ring onto the C atom of Graphene with a distance of 5.88Å and the E_{ad}= -2.551 kcal/mol, which shows that adsorption is weak with ΔEg= - 0.22%.

EA adsorption onto the Si-, Al- and Ga-doped Graphene

Si-doped Graphene

The C atom of the graphene was replaced with the Si atom to find a highly sensitive nanostructure and the new structure was optimized. The geometric structures and properties of Si-doped graphene are investigated and the Density of the State (DOS) plot is shown in Fig. 6. Due to the greater radius of the Si atom than the C atom, the Si atom is placed outside the surface of the nanostructure. The distance

Table 1. Energy of HOMO, LUMO, HOMO-LUMO gap (E_g) in eV, and the change of E_g up on the ethionamide drug adsorption on the graphene nanostructures. The adsorption energy (E_{ad}) is in kcal/mol. %ΔE_g indicates the percentage of the change of E_g after the drug adsorption.

Structure	E_{ad} (kcal/mol)	E_{HOMO} (eV)	E_{LUMO}(eV)	E_g(eV)	%ΔE_g
Geraphene	-------	-4.93	-2.10	2.82	-------
Complex-S	-2.552	-5.10	-2.30	2.75	-1.02%
Complex-N(NH2)	-2.522	-5.14	-2.32	2.81	-0.23%
Complex-N(ring)	-2.551	-5.13	-2.320	2.81	-0.22%

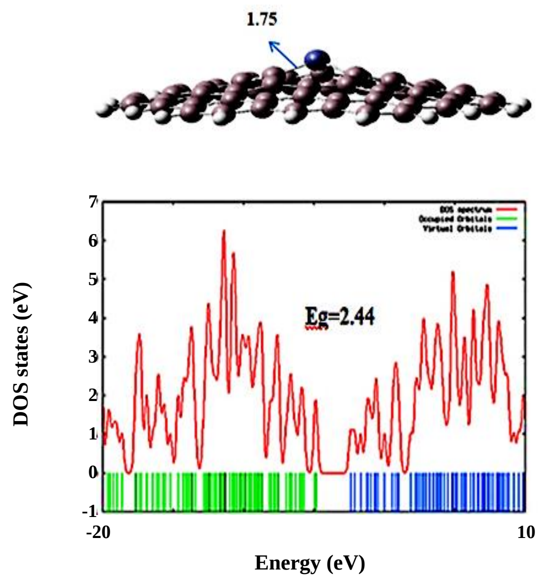

Fig. 6: Optimized structures of Si-doped graphene. Distances are in Å and Density of State (DOS) plot.

of the Si-C of the nanostructure is 1.75 Å. After doping with Si, the HOMO decreases slightly from -4.93 in the pristine graphene to -4.83 eV in the Si-doped graphene while the LUMO increases from -2.10 in the pristine graphene to -2.39 eV in the Si-doped graphene. The E_g changes slightly from 2.82eV in the pristine graphene to 2.44 eV in the Si-doped graphene. According to DFT calculations, Si-doped graphene increases electrical conductivity and it becomes a semiconductor compared to pristine graphene (Table 2).

Si-doped Graphene-EA complex

Since graphene sheets are chemically neutral, placing an element such as the Si atom into graphene will greatly affect the chemical reactivity and properties of graphene. In this case, the interactions between EA and Si-doped graphene are investigated. Three types of complexes were found that indicate interactions between C=S, -NH_2, and N(ring) in EA and the Si atom of Si-doped graphene (Fig. 7 and Table 2). The corresponding density of state (DOS) is also shown in Fig. 12. In the strongest interaction and the most stable complex, the Si atom of Si-doped graphene interacts from the N(ring) head of EA with E_{ad} of -14.83 kcal/mol with the Si….N(ring) distance of 2.02 Å. The HOMO changes from -4.83 in the Si-doped graphene to -4.14eV in the Si-doped graphene-EA complex and the LUMO changes from -2.39 to -3.15eV. The HOMO remains unchanged on the surface of the graphene while the LUMO is localized on the EA atoms which partly transfer to the Si-doped graphene in the complex. The E_g decreased mainly from 2.44eV to 0.98eV and the rate change is ΔE_g= -59.61% which shows the high sensitivity of the Si-doped graphene to the absorption of EA. The high change in E_g is suitable for the sensing ability, lower in E_g significantly increases the electrical conductivity of the nanoparticles which can be converted into an electrical signal, which is related to the presence of drug molecules. The E_{ad}, of -14.83 kcal/mol is suitable that the Si-doped graphene suitable adsorbs EA, which shows that the recovery time is suitable. Therefore, the Si-doped graphene-EA complex is a suitable sensing device. As shown, a suitable sensing ability with respect to higher % ΔE_g indicates the high sensitivity of Si-doped graphene to the EA drug which also confirmed the suitable E_{ad} and recovery time for EA.

In the Si-Complex-S, the EA drug is adsorbed from the S head onto the Si atom of Si-doped graphene at a distance of 2.41 Å. The adsorption energy is -10.83 kcal/mol, indicating weak adsorption, ΔE_g = -44.83% (Fig. 7).

In the Si-Complex-N(NH2), the EA drug is adsorbed from the N(NH_2) atom onto the Si atom of Si-doped graphene with a distance of 4.43 Å. The adsorption energy is -3.27 kcal/mol, indicating weak adsorption, ΔE_g = -0.26 % (Fig. 7).

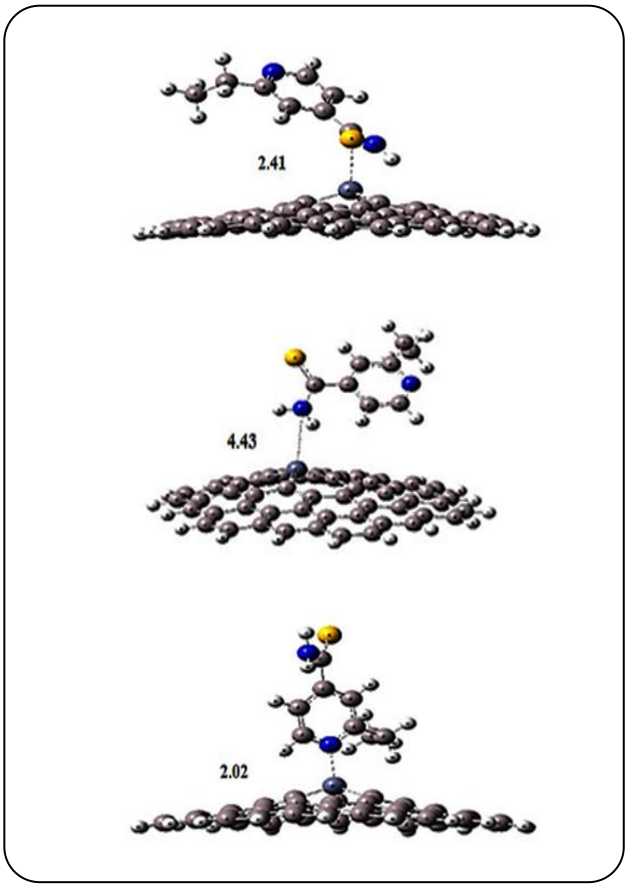

***Fig. 7:** Optimized structures of Si-doped graphene-EA complexes. Distances are in Å.*

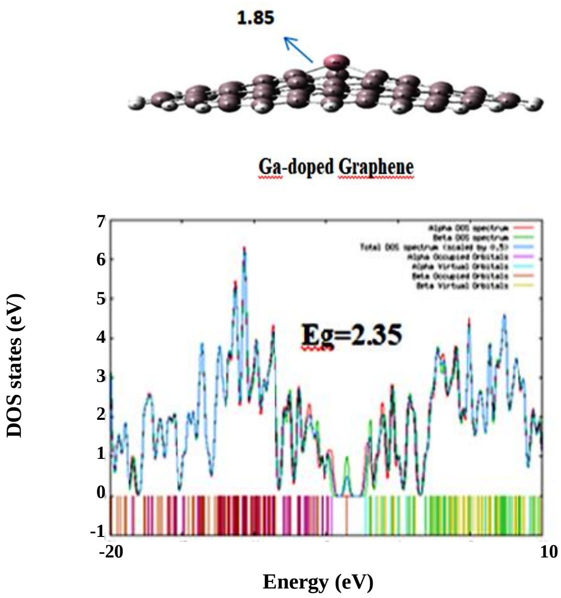

***Fig. 8:** Optimized structures of Ga-doped graphene nanostructures. Distances are in Å and density of state (DOS) plot.*

Ga-doped Graphene

The C atom of graphene was replaced with the Ga atom to find a highly sensitive nanostructure and the new structure was optimized. The geometric structure and properties of Ga-doped graphene are investigated and the Density of State plot (DOS) for the nanostructure is shown in Figure. 8. Due to the larger radius of Ga compared to the C atom, the Ga atom is placed out of the nanostructure surface. The distance of the Ga-C of the graphene is 1.85 A^0. After doping with the Ga atom, the HOMO decreases from -4.93 in the pristine graphene to -4.60 eV in the Ga-doped graphene while LUMO slightly increases from -2.10 in the pristine graphene to -2.25 eV in the Ga-doped graphene. The E_g changed from 2.82 eV in the pristine graphene to 2.35 eV in the Ga-doped graphene. According to DFT calculations, Ga-doped graphene increases the electrical conductivity and it becomes a semiconductor compared to pristine graphene (Table 2).

Ga-doped Graphene-EA complex

Here, the interactions between EA and Ga-doped graphene are investigated. Three types of complexes were found that indicate the interactions between C=S, $-NH_2$, and N-ring in EA and the Ga atom of Ga-doped graphene (Fig.9 and Table 2). The Density of the State (DOS) plot is shown in Fig. 12. In the strongest interaction and the most stable complex, the Ga atom of Ga-doped graphene interacts from the N(ring) head of EA by E_{ad} of -36.66 kcal/mol with a Ga….N(ring) distance of 2.02 Å. The HOMO changes from -4.60 in the Ga-doped graphene to -4.05eV in the Ga-doped graphene-EA complex while the LUMO changes from -2.25 to -2.94 eV. The HOMO remains unchanged on the graphene surface while the LUMO is localized on the EA atoms which partly transfer to the Ga-doped graphene in the complex. The E_g decreased significantly from 2.35 to 1.11eV and the rate of change is ΔE_g = -52.75% which shows the high sensitivity of Ga-doped graphene to the adsorption of EA. Despite the significant change in E_g and the high sensitivity which are suitable for the sensing ability, the E_{ad} of -36.66 kcal/mol is so high that the Ga-doped graphene strongly adsorbs EA, which shows that the recovery time is high, So, the Ga-doped graphene has a suitable sensing ability with respect to a higher $\%\Delta E_g$. However, a higher E_{ad} makes the Ga-doped graphene is a suitable sensing device only at higher temperatures. As mentioned above, due to

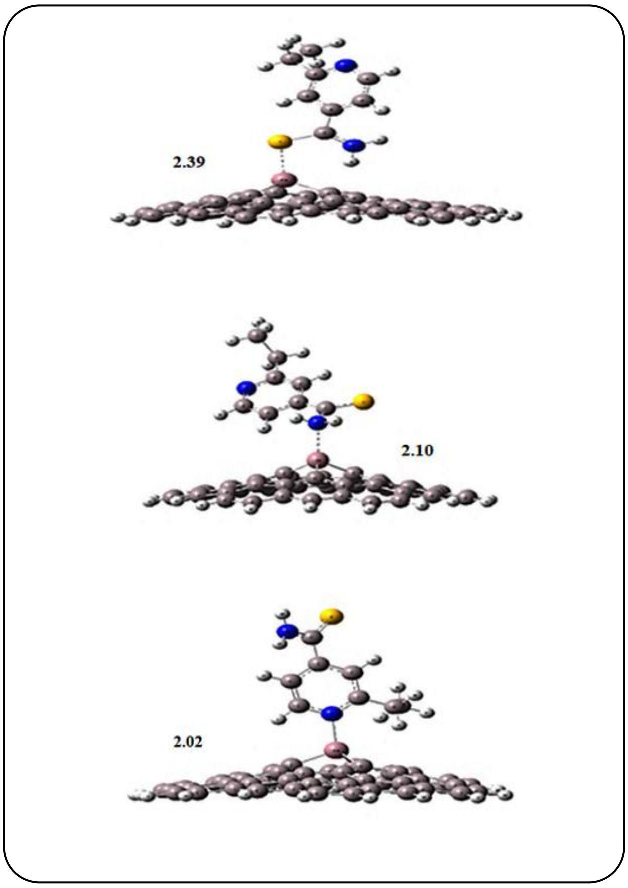

Fig. 9: Optimized structures of Ga-doped graphene-EA complexes. Distances are in Å.

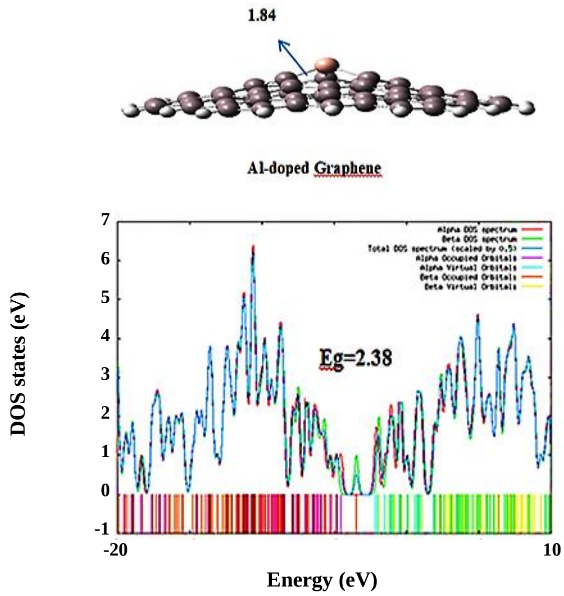

Fig. 10: Optimized structures of Al-doped graphene nanostructures. Distances are in Å and Density of State (DOS) plot.

the adsorption energy of -36.66 kcal/mol and the rather long recovery time, a strong interaction is not suitable for a sensor because the adsorption of EA onto Ga-doped graphene would be difficult. Recovery time is too long and therefore can help to break down and remove this compound.

In the Ga-Complex S, the EA drug is adsorbed from the S atom onto the Ga atom of Ga-doped graphene at a distance of 2.39 A^0. The adsorption energy is -26.13 kcal/mol with ΔE_g= -45.99 % (Fig. 9).

In the Ga-Complex-N(NH2), the EA drug is adsorbed from the N(NH_2) atom onto the Ga atom of Ga-doped graphene with a distance of 2.10 A^0. The adsorption energy is -15.94 kcal/mol, with ΔE_g= -54.98% (Fig. 9).

Al-doped Graphene

The C atom of the graphene was replaced with the Al atom in order to find a highly sensitive nanostructure and the new structure was optimized. The geometric structures and properties of Al-doped graphene are investigated and the Density of State (DOS) plot for the nanostructure is shown in Fig. 10. Due to the larger radius of Al compared to the C atom, the Al atom is placed out of the nanostructure surface. The distance of the Al-N of the nanostructure is 1.84 Å. After doping with Al, the HOMO decreases from -4.93 to -4.53eV in the Al-doped graphene, whereas the LUMO slightly increases from -2.10 in the pristine graphene to -2.14 eV in the Al-doped graphene. The E_g changed from 2.82eV in the pristine graphene to 2.38eV in Al-doped graphene. According to DFT calculations, Al-doped graphene increases the electrical conductivity and it becomes a semiconductor compared to the pristine graphene (Table 2).

Al-doped Graphene-EA complex

Here, the interactions between EA and the Al-doped graphene are investigated. Three types of complexes were found that indicate the interactions between C=S, -NH_2, and N-ring in EA and the Al atom of Al-doped graphene (Fig. 11 and Table 2). The Density of State (DOS) plot is also shown in Fig. 12. In the strongest interaction and the most stable complex, the Al atom of Al-doped graphene interacts from the N(ring) head of EA with E_{ad} of -34.53 kcal/mol with the Al…N(ring) distance of 2.03Å. The high adsorption energy in the Al-doped graphene-EA complex may be due to the greater curvature of the pristine graphene. The HOMO changes from -4.53 in the Al-doped

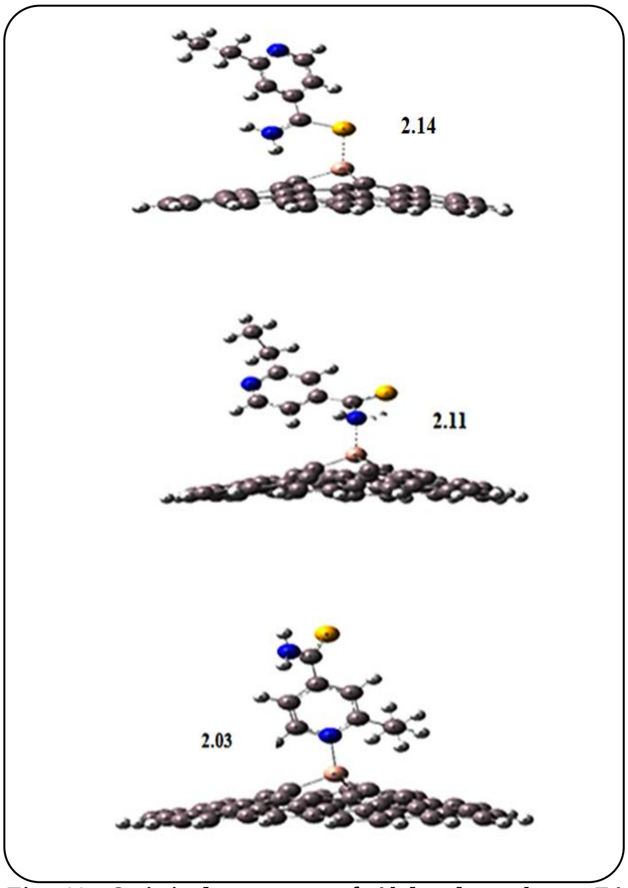

***Fig. 11:** Optimized structures of Al-doped graphene -EA complexes. Distances are in Å.*

graphene to -4.05eV in the Al-doped graphene -EA complex and the LUMO changes from -2.14 to -3.07eV. The HOMO remains unchanged on the graphene surface, while LUMO is localized on EA atoms which partly transfer to the Al-doped graphene in the complex. The E_g decreased significantly from 2.38 to 0.97 eV and the rate of change is ΔE_g= -58.98% which shows the high sensitivity of Al-doped graphene to the adsorption of EA. The E_{ad} of -34.53 kcal/mol is so high that the Al-doped graphene strongly adsorbs EA, which shows that the recovery time is high, So the Al-doped graphene has a suitable sensing ability with respect to a higher %ΔE_g. However, a higher E_{ad} makes the Al-doped graphene a suitable sensing device only at higher temperatures. As mentioned, due to the adsorption energy of -34.53 kcal/mol and the rather long recovery time, the strong interaction energy between the Al-doped graphene and EA is not suitable for a sensor because the EA desorption on the Al-doped graphene will be difficult. A system with high adsorption energy can be a sensor at

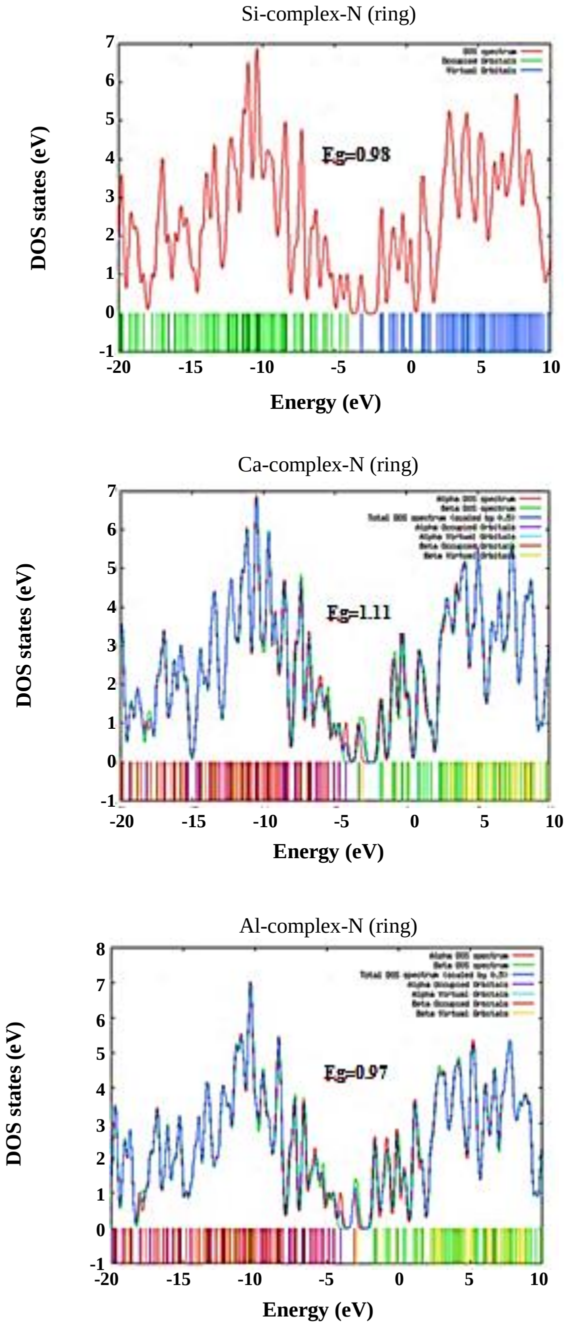

***Fig. 12:** Density of states (DOS) plots of (a) Si-Complex-N(ring), (b) Ga-Complex-N(ring), (c) Al-Complex-N(ring).*

high temperatures, because at high temperatures the recovery time is reduced.

In the Al-Complex-N(NH2), EA is adsorbed from the N head of NH2 onto the Al atom of Al-doped graphene with a distance of 2.11Å. The adsorption energy is -16.50 kcal/mol, indicating weak adsorption, ΔE_g= -63.67% (Fig. 11).

Table 2: Energy of HOMO, LUMO, HOMO-LUMO gap (Eg) in eV, and the change of Eg upon the Ethionamide drug adsorption on the Si and Ga, Al-doped graphene nanostructures. The adsorption energy (Ead) is in kcal/mol. %ΔEg indicates the percentage of the change of Eg after the Ethionamide adsorption.

Structure	E_{ad} (kcal/mol)	E_{HOMO} (eV)	E_{LUMO}(eV)	E_g(eV)	%ΔE_g
Si-Geraphene	-------	- 4.83	- 2.39	2.44	-------
Si-Complex-S	-10.83	- 4.30	-2.95	1.34	-44.83%
Si-Complex-N(NH2)	-3.27	-5.04	-2.61	2.43	-0.26%
Si-Complex-N(ring)	-14.83	-4.14	-3.15	0.98	-59.61%
Ga-Graphene	-------	-4.60	-2.25	2.35	-------
Ga-Complex-S	-26.13	-4.13	-2.86	1.27	-45.99%
Ga-Complex-N(NH2)	-15.94	-4.23	-3.17	1.05	-54.98%
Ga-Complex-N(ring)	-36.66	-4.05	-2.94	1.11	-52.75%
Al-Geraphene	-------	-4.53	-2.14	2.38	-------
Al-Complex-S	-28.90	-4.13	-2.95	1.17	-50.63%
Al-Complex-N(NH2)	-16.50	-4.22	-3.36	0.86	-63.67%
Al-Complex-N(ring)	-34.53	-4.05	-3.07	0.97	-58.98%

In the Al-Complex-S, EA is adsorbed from the S onto the Al atom of Al-doped graphene with a distance of 2.14 Å. The adsorption energy is -28.90kcal/mol, indicating suitable adsorption with ΔE_g= -50.63% (Fig. 11). It is obvious that in the theoretical studies, the mathematical parameters help to improve our research works [110-129].

CONCLUSIONS

In this research, the energy of interactions and the sensing ability between EA and the pristine, Si- and Ga- and Al-doped graphene has been studied by using density functional theory (DFT) calculations. Also, the adsorption behavior of pristine graphene, Si- and Ga- and Al-doped graphene has been investigated toward EA. The E_{ad} of the pristine graphene-EA complex in the most stable complex-S is -2.552 kcal/mol which is weak, it is physical adsorption and this system seems not suitable for potential sensing. The E_g for the Si-doped graphene-EA complex decreased from 2.44eV to 0.98eV and the rate of change is ΔE_g= -59.61% which shows the high sensitivity of the Si-doped graphene to the adsorption of EA. The adsorption energy of -14.83 kcal/mol is suitable which shows that the recovery time is suitable, and can be used as suitable sensing. The E_g for Ga-doped graphene-EA complex decreased significantly from 2.35 to 1.11eV and the rate of change is ΔE_g= -52.75%, which shows the high sensitivity of the Ga-doped graphene to the adsorption of EA. Despite the high sensitivity, the adsorption energy of -36.66 kcal/mol is high which shows that the Ga-doped graphene-EA complex can be used as a suitable sensing device only at higher temperatures.The E_g for the Al-doped graphene-EA complex decreased significantly from 2.38 to 0.97eV and the rate of change is ΔE_g= -58.98% which indicates the high sensitivity of the Al-doped graphene to the adsorption of EA. The E_{ad} of -34.53 kcal/mol is high which shows that the Al-doped graphene-EA complex can be used as a suitable sensing device only at higher temperatures.

Received : Sep. 15, 2021 ; Accepted : Dec. 12, 2021

REFERENCES

[1] Sayadi M.H., Trivedy R.K., Pathak R.K., Pollution of Pharmaceutical in Environment, *J. Industr. Pollut. Control*, **26(1)**: 89-94 (2010).

[2] Aherne G.W., English J., Marks V., The Role of Immuno Assay in the Analysis of Micro Contaminants in Water Samples, *Ecotoxicol. Environ*, **9(1)**: 79-83 (1985).

[3] Dietrich D.R., Webb S.F., Petry T., Hot Spot Pollutants: Pharmaceuticals in the Environment, *Toxicology. Letters*, **131(1-2)**: 1-3 (2002).

[4] Webb S.F., "A Data Based Perspective on the Environmental Risk Assessment of Human Pharmaceuticals II Aquatic Risk Characterization, In Pharmaceuticals in the Environment: Sources, Fate, Effects and Risks", K. Kummerer, Ed, Springer-Verlag, Berlin, Heidelberg, Germany, 203-219 (2001).

[5] Petrovic M., Gonzalez S., Barcelo D., Analysis and Removal of Emerging Contaminants in Waste Water and Drinking Water, *Trends. Anal. Chem*, **22(10)**: 685–696 (2003)

[6] Jones O.A.H., Voulvoulis N., Lester J.N., Human Pharmaceuticals in the Aquatic Environment: A Review, *Environ. Technol*, **22(12)**: 1383-1394 (2001).

[7] Sayadi M.H., "Contamination of Soil in Industrial Area", Lambert. Academic. Publishing, Germany, 156 (2010).

[8] Zuccato E., Calamari D., Natangelo M., Fanelli R. Presence of Therapeutic Drugs in the Environment, *Lancet*, **355(9217)**: 1789-90 (2000).

[9] Baran W., Adamek E., Ziemia-Nska J., Sobczak A., Effects of The Presence of Sulfonamides in the Environment and Their Influence on Human Health, *J. Hazard. Mater*, **196**: 1-15 (2011).

[10] Białk- Bielinska A., Stolte S., Arning J., Uebers U., Boschen A., Stepnowski P., Matzke M,. Ecotoxicity Evaluation of Selected Sulfonamides, *Chemosphere*, **85(6)**: 928–933 (2011).

[11] Berdinsky A.S., Shevtsov Y.V., Okotrub A.V., Trubin S.V., Chadderton l.t., Fink D., Lee J., Sensor Properties of Fullerene Films and Fullerene Compounds with Iodine, *Chem. Sustain. Develop*, **8**: 141-146 (2000).

[12] Peyghan A.A., Moradi M., First-Principle Study of Methanol Adsorption on Ni(Pd)-Decorated Graphene, *J. Iran. Chem. Soc.*, **12**: 751-756 (2015).

[13] Oku ., Kuno M., Kitahara H., Narita L., Formation Atomic Structures and Properties of Boron Nitride and Carbon Nanocage Fullerene Materials, *International. J. Inorgan. Mater*, **3(7)**: 597-612 (2001).

[14] Choi W., Lahiri I., Seelaboyina R., Kang Y.S., Synthesis of Graphene and Its Applications: A Review, Critical Reviews in Solid State and Materials Sciences, *Taylor & Francis*, **35(1)**: 52-71 (2010).

[15] Whitener K.E., Sheehan P.E., Graphene synthesis, *Diamond. Relat. Mater*, **46**: 25-34 (2014).

[16] Singh V., Joung D., Zhai L., Das S., Khndakero S.I., Seal S., Graphene Based Materials: Past, Present and Future, *Prog. Mater. Sci*., **56(8)**: 1178-1271 (2011).

[17] Novoselov K.S., Geim A.K., Morozov S.V., Jiang M., Katsnelson., Grigorieva I.V., Dubonos S.V., Firsov A.A., Two-Dimensional Gas of Massless Dirac Fermions in Graphene, *J. Refere. Nature*, **438 (7065)**:197–200 (2005).

[18] Ghiasi M., Zeinali P., Gholami S., Zahedi M., Separation of CH_4, H_2S, N_2 and CO_2 Gases Using Four Types of Nanoporous Graphene Cluster Model: a Quantum Chemical Investigation, *J. Mol. Model*, **27**: 201 (2021).

[19] Mohammad Hosein A.S., Jamehbozorgi S., Beheshtian J., Investigation of Interaction Between Graphene and Its Compounds as Carrier on Anti-Cancer Drug of 5-Fluorouacil, *Eur. J. Chem*, **13(3)**: 28 (2018).

[20] Rahmani Z., Edjlali L., Vessally E., Hosseinian A., Kheirollahi Nezhad P., A DFT Study on the Sulfanilamide Interaction with Graphene-like Boron nitride Nano Sheets, *J. Sulfur. Chem*., **41(5)**: 483-497 (2020).

[21] Schmidt M., Baldridge K., Boatz J., et al., General Atomic and Molecular Electronic Structure System, *J. Comput. Chem*, **14**: 1347–1363 (1993).

[22] Nagarajan V., Chandiramouli R., TeO_2 Nano Structures as a NO_2 Sensor: DFT Investigation, *Comput. Theorei. Chem*, **1049**: 20-27 (2014).

[23] Tabtimsai C., Ruangpornvisuti V., Wanno B., Density Functional Theory Investigation of the VIIIB Transition Metal Atoms Deposited on (5, 5) Single-Walled Carbon Nanotubes, *Physica. E*, **49**: 61-67 (2013).

[24] Zhou W., Zhou J., Shen J., Ouyang C., Shi S., First-Principles Study of High-Capacity Hydrogen Storage on Graphene with Li Atoms, *J. Physics. Chem. Solids*, **73(2)**: 245-251 (2012).

[25] Mohammadi S., Musavi M., Abdollahzadeh F., Babadoust SH., Hosseinian A., Application of NanoCatalysts in C-Te Cross-coupling Reactions: An Overview, *Chem. Rev. Lett*, **1**: 49–55 (2018).

[26] Beheshtian J., Peyghan A.A., Bagheri Z., Detection of Phosgene by Sc-Doped BN Nanotubes: A DFT Study, *Sens. Actuators B. Chem*, **171**:846–852 (2012).

[27] Samadizadeh M., Rastegar S.F., Peyghan A.A., F−, Cl−, Li+ and Na+ Adsorption on AlN Nanotube Surface: a DFT Study, *Physica. E*, **69**:75–80. (2015).

[28] Behmagham F., Asadi Z., Jamal Sadeghi Y., Synthesis, Spectroscopic and Computational Investigation of Bis (3-methoxyphenylthio) ethyl) Naphthalene. *Chem. Rev. Lett.* **1**:68–76 (2018).

[29] Babanezhad E., Beheshti A. The Possibility of Selective Sensing of the Straight-Chain Alcohols (Including Methanol to n-pentanol) by Using the C20 Fullerene and C18NB Nano Cage, *Chem. Rev. Lett.* **1**:82–88 (2018).

[30] Baughman R.H., Zakhidov A.A., De Heer W.A., Carbon Nanotubes--the Route Toward Applications, *Science*, **297**: 787-792 (2002).

[31] Pop E., Mann D., Wang Q., Goodson K., Dai H., Thermal Conductance of an Individual Single-Wall Carbon Nanotube Above Room Temperature, *Nano. Lett.*, **6**: 96-100 (2006).

[32] Parr R.G., "Density Functional Theory of Atoms and Molecules:, In: Fukui K, Pullman B, Editors. "Horizons of Quantum Chemistry". Dordrecht: Académie Internationale Des Sciences Moléculaires Quantiques / International Academy of Quantum Molecular Science (1980).

[33] OBoyle N., Tenderholt A., Langner K., A Library for Package Independent Computational Chemistry Algorithms, *J. Comput. Chem*, **29(5)**: 839-845 (2008).

[34] Boys S.F., Bernardi F., The Calculation of Small Molecular Interactions by Differences of Separate Total Energies - Some Procedures with Reduced Errors, J. *Molecul. Physics*, **19(4)**: 553-561 (1970).

[35] Heravi M. R.P., Habibzadeh S., Ebadi A. G., Kheirollahi Nezhad P.D., Vessally E., Substituent Effects of Fused Hammick Silylenes *via* Density Functional Theory Survey, *J. Phys. Org. Chem*, **34(11):** 4264 (2021).

[36] Ma X., Kexin Z., Yonggang W., Ebadi A. G., Toughani M., Investigation of Low-Temperature Lipase Production and Enzymatic Properties of Aspergillus Niger, *Iran. J. Chem. Chem. Eng. (IJCCE)*, **49(4):** 1364-1374 (2021).

[37] Soleimani-Amiri S., Asadbeigi N., BadraghehbS., A Theoretical Approach to New Triplet and Quintet (nitrenoethynyl) alkylmethylenes,(nitrenoethynyl) alkylsilylenes,(nitrenoethynyl) alkylgermylenes, *Iran. J. Chem. Chem. Eng. (IJCCE)*, **39(4)**: 39-52 (2020).

[38] Zandieh S., Nami N., Hossaini Z., Ionic Liquid an Efficient Solvent and Catalyst for Synthesis of 1- aminoalkyl-2-naphthol and Naphthoxazine Derivatives, *Iran. J. Chem. Chem. Eng. (IJCCE)*, **38(4)**: 27-35 (2019).

[39] Ahmadi S., Hosseinian A., Delir Kheirollahi Nezhad P., Monfared A., Vessally E., Nano-Ceria (CeO_2): An Efficient Catalyst for the Multi-Component Synthesis of a Variety of Key Medicinal Heterocyclic Compounds, *Iran. J. Chem. Chem. Eng. (IJCCE)*, **38(6)**: 1-19 (2019).

[40] Vessally E., Mohammadi S., Abdoli M., Hosseinian A., Ojaghloo P., Convenient and Robust Metal-Free Synthesis of Benzazole-2-Ones Through the Reaction of Aniline Derivatives and Sodium Cyanate in Aqueous Medium, *Iran, J. Chem. Chem. Eng. (IJCCE)*, **39(5)**: 11-19 (2020).

[41] Jalali Sarvestani M.R., Fullerene P., (C20) as a Potential Adsorbent and Sensor for the Removal and Detection of Picric Acid Contaminant: DFT Studies Charehjou, Cent, *Asian J. Environ. Sci. Technol. Innov*, **2:** 12-19 (2021).

[42] Heravi M.R.P., Hosseinian A., Rahmani Z., Ebadi A., Vessally E., Transition- Metal- Catalyzed Dehydrogenative Coupling of Alcohols and Amines: a Novel and Atom- Economical Access to Amides, *J. Chin. Chem. Soc*, **68(5):** 723-737(2021).

[43] Xu W., Guo D., Ebadi A. G., Toughani M., Vessally E., Transition-Metal Catalyzed Carboxylation of Organoboron Compounds with CO_2, *Journal of CO_2 Utilization*, **45**: 101403 (2021).

[44] Hassanpour A., Heravi M. R. P., Ebadi A., Hosseinian A., Vessally E., Oxidative Trifluoromethyl (thiol/selenol) ation of Terminal Alkynes: An Overview, *Journal of Fluorine Chemistry*, 109762 (2021).

[45] Kareem R.T., Azizi B., Asnaashariisfahani M., Ebadi A., Vessally E., Vicinal Halo-Trifluoromethylation of Alkenes, *RSC Advances*, **11(25)**: 14941-14955 (2021).

[46] Azizi B., Heravi M.R.P., Hossaini Z., Ebadi A., Vessally E., Intermolecular Difunctionalization of Alkenes: Synthesis of Β-Hydroxy Sulfides, *RSC Adv.*, **11**: 13138-13151(2021).

[47] Xu W., Ebadi A. G., Toughani M., Vessally E., Incorporation of CO2 into Organosilicon Compounds *via* Csi Bond Cleavage, *J. CO_2. Utili*, 101358 (2020).

[48] Liu Z., Ebadi A., Toughani M., Mert N., Vessally E., Direct Sulfonamidation of (Hetero)Aromatic C–H Bonds with Sulfonyl Azides: A Novel and Efficient Route to N-(Hetero)Aryl Sulfonamides, *RSC. Adv*, **10**: 37299-37313 (2021).

[49] Liu Y., Ebadi A. G., Youseftabar-Miri L., Hassanpour A., Vessally E., Methods for Direct C (sp 2)–H Bonds Azidation, *RSC Advances*., **9(43)**: 25199-25215 (2019).

[50] Rasouli A., Bafkar A., Chaghakaboodi Z., Kinetic and Equilibrium Studies of Adsorptive Removal of Sodium-Ion onto Wheat Straw and Rice Husk Wastes, *Sci. Technol. Innov*., **1**: 310-329 (2020).

[51] Ali A., Iqbal M., Waheed A., Co-Treatment of Chlorophenol and Methanolic Wastes, *Central Asian Journal of Environmental Science and Technology Innovation*., **1(5)**: 277-280 (2020).

[52] (a) Jalali Sarvestani M., Mert N., Vessally E., Cross-Dehydrogenative Coupling of Aldehydes with N-Hydroxyimides: An Efficient and Straightforward Route to N-Hydroxyimides Esters, *J. Chem. Lett*, **1(3):** 93-102 (2020).

(b) Vessally E., Behmagham F., Metal-Free Regioselective Thiocyanation of (Hetero) Aromatic C-H Bonds Using Ammonium Thiocyanate: *Overview*. *J. Chem. Lett.*, **1**: 25-31(2020).

(c) Abdulkareem Mahmood E., Azizi B., Majedi S., Decarboxylative Cyanation and Azidation of Carboxylic Acids: an Overview, *Chem. Rev. Lett.*, **3(1)**: 2-8 (2020).

(d) Salehi N., Azizi B., Electrochemical Double Carboxylation of Unsaturated C-C Bonds with Carbon Dioxide: An Overview, *J. Chem. Lett..*, **2(1)**: 2-8 (2021).

(e) Tayde D., Lande M., Synthesis of 2, 4 Disubstituted 1, 5 Benzodiazepines Promoted by Efficient Silica-Alumina Catalyst, *Chem. Rev. Lett*, **4(1)**: 30-36 (2021).

(f) Bakhtiary A., Heravi M.R.P., Hassanpour A., Amini I., Vessally E., Recent Trends in the Direct Oxyphosphorylation of C–C Multiple Bonds, *RSC. Adv*, **11**, 470-483 (2021).

[53] Sreerama L., Vessally E., Behmagham F., Oxidative Lactamization of Amino Alcohols: An Overview, *J. Chem. Lett*, **1**: 9-18 (2020).

[54] (a) Majedi S., Behmagham F., Vakili M., Theoretical View on Interaction Between Boron Nitride Nanostructures and Some Drugs, *J. Chem. Lett*, **1(1)**: 19-24 (2020).

(b) Jalali Sarvestani M., Majedi S., A DFT Study on the Interaction of Alprazolam with Fullerene (C20), *J. Chem. Lett*, **1(1)**: 32-38 (2020).

(c) Kamel M., Morsali A., Raissi H., Mohammadifard K., Theoretical Insights into the Intermolecular and Mechanisms of Covalent Interaction of Flutamide Drug With COOH and COCL Functionalized Carbon Nanotubes: A DFT Approach, *Chem. Rev. Lett*, **3(1)**: 23-37 (2020).

(d) Jalali Sarvestani M., Ahmadi R., Farhang Rik B., Procarbazine Adsorption on The Surface of Single Walled Carbon Nanotube: DFT Studies, *Chem. Rev. Lett.*, **3(4)**: 175-179 (2020).

(e) Jalali Sarvestani M., Doroudi Z., Fullerene (C20) as a Potential Sensor for Thermal and Electrochemical Detection of Amitriptyline: A DFT Study, *J. Chem. Lett*, **1(2)**: 63-68 (2020).

[55] Rani V.A., Prabhakaran D., Thirumarimurugan M.,. Modelling And Control of Ph in a Continuous Stirred Tank Reactor (Cstr), *J. Environ. Prot. Ecol.*, **21(2)**: 413-422 (2020).

[56] Ma X., Kexin Z., Yonggang W., Ebadi A.G., Toughani M., Investigation of Low-Temperature Lipase Production and Enzymatic Properties of Aspergillus Niger, *Iran. J. Chem. Chem. Eng. (IJCCE)*, **40(4)**: 1364-1374 (2021).

[57] Liu W., Zhang H., Gong J., Liu J., Advanced Treatment of Dyed Wastewater from Papermaking with Wastepaper Based on the Fenton Method, *J. Environ. Prot. Ecol.*, **21(2)**: 433-442 (2020).

[58] Soleimani-Amiri, S., Asadbeigi, N., & Badragheh, S., A Theoretical Approach to New Triplet and Quintet (nitrenoethynyl) alkylmethylenes,(nitrenoethynyl) alkylsilylenes,(nitrenoethynyl) alkylgermylenes, *Iran. J. Chem. Chem. Eng. (IJCCE)*., **39(4)**: 39-52 (2020).

[59] Soceanu A., Dobrinas S., Popovici I.C., Jitariu D., Health Risk Assessment of Heavy Metals in Seafood, *J. Environ. Prot. Ecol.*, **21(2)**: 490-497 (2020).

[60] Ahmadi, S., Hosseinian, A., Delir Kheirollahi Nezhad, P., Monfared, A., Vessally, E., Nano-Ceria (CeO2): An Efficient Catalyst for the Multi-Component Synthesis of a Variety of Key Medicinal Heterocyclic Compounds, *Iran. J. Chem. Chem. Eng. (IJCCE)*., **38(6)**: 1-19 (2019).

[61] Burlacu I.F., Favier L., Matei E., Predescu C., Deák G., Photocatalytic Degradation of a Refractory Water Pollutant Using Nanosized Catalysts, *J. Environ. Prot. Ecol.*, **21(2)**: 571-578 (2020).

[62] Vessally E., Mohammadi S., Abdoli M., Hosseinian A., Ojaghloo P., Convenient and Robust Metal-Free Synthesis of Benzazole-2-Ones Through the Reaction of Aniline Derivatives and Sodium Cyanate in Aqueous Medium, *Iran. J. Chem. Chem. Eng. (IJCCE)*., **39(5)**: 11-19 (2020).

[63] Su D., Jing W., Intelligent Pid Driving and Control in the Centrifugal Microfluidic Chip Environment, *J. Environ. Prot. Ecol.*, **21(2)**: 644-653 (2020).

[64] Paduretu C.C., Apetroaei M.R., Apetroaei G.M., Atodiresei D., Rau I., Dyes Adsorption by Using Different Types of Chitosan for Decontamination of Cleaning Waters from Chemical Carriers, *J. Environ. Prot. Ecol.*, 21(1): 28-36 (2020).

[65] Jalali Sarvestani M.R., Charehjou P., Fullerene (C20) as a Potential Adsorbent and Sensor for the Removal and Detection of Picric Acid Contaminant: DFT Studies, *Central Asian Journal of Environmental Science and Technology Innovation*, **2(1)**: 12-19 (2021).

[66] Rekha, K., Thenmozhi, D.R., Characterisation and Utilisation of Sugarcane Bagasse Ash as Pozzolanic Material and Its Effect on Mechanical Strength of Concrete, *J. Environ. Prot. Ecol.*, **21(1)**: 268-279 (2020).

[67] Gharibzadeh F., Vessally E., Edjlali L., Es' haghi M., Mohammadi R., A DFT Study on Sumanene, Corannulene and Nanosheet as the Anodes in Li−Ion Batteries, *Iran. J. Chem. Chem. Eng. (IJCCE)*, **39**: 51-62 (2020).

[68] Cani, X.H., Malollari, I., Nuro, A. And Buzo, R., Classification of Hydrocarbons Content in Used Tyres Pyrolytic Oil, by Gas Chromatography Method, *J. Environ. Prot. Ecol.*, **21(1)**: 300-307 (2020).

[69] Vessally E., Hosseinian A., A Computational Study on the Some Small Graphene-Like Nanostructures as the Anodes in Na−Ion Batteries, *Iran. J. Chem. Chem. Eng. (IJCCE)*, **40**: 691-703 (2021).

[70] Hornet M., Cirstolovean I.L., Nastac D.C., Todor R., Natural Ventilation for Amphitheatres-A Way of Increasing Indoor Air Quality by Decreasing Energy Consumption, *J. Environ. Prot. Ecol.*, **21(1)**: 10-18 (2020).

[71] Vessally E., Farajzadeh P., Najafi E., Possible Sensing Ability of Boron Nitride Nanosheet and Its Al– and Si–Doped Derivatives for Methimazole Drug by Computational Study, *Iran. J. Chem. Chem. Eng. (IJCCE)*, **40(4)**: 1001-1011 (2021).

[72] Ivanova L.P., Vassileva P.S., Gencheva G.G., Detcheva A.K., Feasibility of Two Bulgarian Medicinal Plant Materials for Removal of Cu^{2+} Ions from Aqueous Solutions, *J. Environ. Prot. Ecol.*, **21(1)**: 37-45 (2020).

[73] Hashemzadeh B., Edjlali L., Delir Kheirollahi Nezhad P., Vessally E., A DFT Studies on a Potential Anode Compound for Li-Ion Batteries: Hexa-Cata-Hexabenzocoronene Nanographen, *Chem. Rev. Lett.*, (2021).

[74] Salehi N., Vessally E., Edjlali L., Alkorta I., Eshaghi M., Nan@Tetracyanoethylene (n=1-4) Systems: Sodium Salt vs Sodium Electrode, *Chem. Rev. Lett.*, **3**: 207-217 (2020).

[75] Sreerama L., Vessally E., Behmagham F., Oxidative Lactamization of Amino Alcohols: An Overview, *J. Chem. Lett.*, **1**: 9-18 (2020).

[76] Majedi S., Sreerama L., Vessally E., Behmagham F., Metal-Free Regioselective Thiocyanation of (Hetero) Aromatic C-H Bonds using Ammonium Thiocyanate: An Overview, *J. Chem. Lett.*, **1**: 25-31 (2020).

[77] Sur I.M., Micle V., Damian G.E., Assessment of Heavy Metal Contamination and Bioremediation Potential of Thiobacillus Ferrooxidans in Soils Around Copper Quarry, *J. Environ. Prot. Ecol.*, **21(1)**: 56-62 (2020).

[78] Shajari N., Yahyaei H., Ramazani A., Experimental and Computational Investigations of Some New Cabamothioate Compounds, *Chem. Rev. Lett.*, **4**: 21-29 (2021).

[79] Majedi, S., Majedi, S., Existing Drugs as Treatment Options for COVID-19: A Brief Survey of Some Recent Results, *J. Chem. Lett.*, **1**: 2-8 (2020).

[80] Jalali Sarvestani M.R., Majedi S., A DFT Study on the Interaction of Alprazolam with Fullerene (C20), *J. Chem. Lett.*, **1**: 32-38 (2020).

[81] Kamel, M., Mohammadifard, K., Thermodynamic and Reactivity Descriptors Studies on the Interaction of Flutamide Anticancer Drug with Nucleobases: A Computational View, *Chem. Rev. Lett.*, **4**: 54-65 (2021).

[82] Majedi, S., Behmagham, F., Vakili, M., Theoretical View on Interaction Between Boron Nitride Nanostructures and Some Drugs, *J. Chem. Lett.*, **1**: 19-24 (2020).

[83] Liu H., Wang Y., Li Q., Yang N., Wang Z., Wang Q., Research on the Evolution Characteristics of Oxygen-Containing Functional Groups During the Combustion Process of the Torrefied Corn Stalk, *Biomass and Bioenergy*., **158**: (2022).

[84] Zhang M., Sun X., Wang C., Wang Y., Tan Z., Li J., Xi B., Photocatalytic Degradation of Rhodamine B Using Bi4O5Br2-doped ZSM-5, *Materials chemistry and physics*., **278**: 125697 (2022).

[85] Jia J., Cao Y., Wu T., Tao Y., Pan Y., Huang F., Tang H., Highly Regio- and Stereoselective Markovnikov Hydrosilylation of Alkynes Catalyzed by High-Nuclearity {Co14} Clusters, *ACS Catalysis*., **11(12)**: 6944-6950 (2021).

[86] Shi C., Wu Z., Yang F., Tang Y., Janus Particles with pH Switchable Properties for High-Efficiency Adsorption of Ppcps in Water, *Solid State Sciences*, **119**: 106702 (2021).

[87] Zhang X., Tang Y., Zhang F., Lee C., A Novel Aluminum-Graphite Dual-Ion Battery, *Advanced Energy Materials*, **6(11)**: 1502588 (2016).

[88] Wang M., Jiang C., Zhang S., Song X., Tang Y., Cheng H., Reversible Calcium Alloying Enables a Practical Room-Temperature Rechargeable Calcium-Ion Battery with a High Discharge Voltage, *Nature chemistry*., **10(6)**: 667-672 (2018).

[89] Mu S., Liu Q., Kidkhunthod P., Zhou X., Wang W., Tang Y., Molecular Grafting Towards High-Fraction Active Nanodots Implanted in N-Doped Carbon for Sodium Dual-Ion Batteries, *National Science Review*, **8(7)**: (2020).

[90] Xiong Q., Chen Z., Huang J., Zhang M., Song H., Hou X., Feng Z., Preparation, Structure and Mechanical Properties of Sialon Ceramics by Transition Metal-Catalyzed Nitriding Reaction, *Rare Metals*, **39(5)**: 589-596 (2020).

[91] Zhu W., Deng M., Chen D., Zhang Z., Chai W., Chen D., Hao Y., Dual-Phase CsPbCl3–Cs4PbCl6 Perovskite Films for Self-Powered, Visible-Blind UV Photodetectors with Fast Response, *ACS Applied Materials & Interfaces*., **12(29)**: 32961-32969 (2020).

[92] Liu H., Li X., Ma Z., Sun M., Li M., Zhang Z., Guo S., Atomically Dispersed Cu Catalyst for Efficient Chemoselective Hydrogenation Reaction, *Nano Letters*, **21(24)**: 10284-10291 (2021).

[93] Yang Y., Wang Y., Zheng C., Lin H., Xu R., Zhu H., Xu X., Lanthanum Carbonate Grafted ZSM-5 for Superior Phosphate Uptake: Investigation of the Growth and Adsorption Mechanism, *Chemical Engineering Journal (Lausanne, Switzerland: 1996)*., **430**: 133166 (2022).

[94] Chen X., Wang D., Wang T., Yang Z., Zou X., Wang P., Wei Z., Enhanced Photoresponsivity of a GaAs Nanowire Metal-Semiconductor-Metal Photodetector by Adjusting the Fermi Level, *ACS Applied Materials & Interfaces*, **11(36)**: 33188-33193 (2019).

[95] Li H., Tang J., Kang Y., Zhao H., Fang D., Fang X., Wei Z., Optical Properties of Quasi-type-II Structure in GaAs/GaAsSb/GaAs Coaxial Single Quantum-Well Nanowires, *Applied Physics Letters*, **113(23)**: 233104 (2018).

[96] Yan W., Cao M., Fan S., Liu X., Liu T., Li H., Su J., Multi-yolk ZnSe/2(CoSe2)@NC Heterostructures Confined in N-Doped Carbon Shell for High-Efficient Sodium-Ion Storage, *Composites. Part B, Engineering*., **213**: 108732 (2021).

[97] Wang G., Liu D., Fan S., Li Z., Su J., High-k Erbium Oxide Film Prepared by Sol-Gel Method for Low-Voltage Thin-Film Transistor, *Nanotechnology*, **32(21)**: 215202 (2021).

[98] Zhao R., Wei X., Zhu H., Li S., Li H., Edge Stabilities and Growth Kinetics of Graphene-Like Two Dimensional Monolayers Composed with Group 15 Elements, *Physical Chemistry Chemical Physics*., (2022).

[99] Kanule J., Ng Etich W., Numerical Modeling of Translational Dynamics for Shallow Landslides. Based on Flume Tests-Special Case of Spherical-Cap-Shaped Slope Sections, *Geology, Ecology, and Landscapes*., **4(2)**: 151-158 (2020).

[100] Chen H., Liu H., Ge H., Kong F., Han Z., Yu D., Mechanics Characteristics of Chamber and Slide System of Vertical Slide Marine Emergency Evacuation System. *Journal of Coastal Research*, **103(sp1)**: 311-317 (2020).

[101] Yao H., Modeling and Dynamics Analysis of Marine Planktonic Ecosystem Based on Adaptive Fuzzy Variable Structure Control Approach. *Journal of coastal research*., **103(sp1)**: 436-441 (2020).

[102] Molla M.A.I., Furukawa M., Tateishi I., Katsumata H., Suzuki T., Kaneco S., Photocatalytic Degradation of Fenitrothion in Water With TiO_2 under Solar Irradiation, *Water Conservation and Management*, **2(2)**: 1-5 (2018).

[103] Om Prakash Singh., Gaurav Kumar., Mukesh Kumar., Role of Taguchi and Grey Relational Method in Optimization of Machining Parameters of Different Materials: A Review. *Acta Electronica Malaysia*., **3(1)**: 19-22 (2019).

[104] Redondo A., Zeiri Y., Low J.J., Goodard W.A., Application of Transition State Theory to Desorption from solid Surfaces: Ammonia on Ni(111), *J. Chem. Physics,* **79**: 6410–6415 (1983).

[105] Kumar R., Goel N., Kumar M., UV-ActivatedMoS2 Based Fast and Reversible NO_2 Sensor at Room Temperature, *ACS. Sensors*, **2(11)**: 1744–1752 (2017).

[106] Bano A., Krishna J., Pandey D.K., Gaur N.K., An Ab Initio Study of Sensing Applications of MoB_2 Monolayer: A Potential Gas Sensor, *Physic. Chem. Chemi. Physics*, **21**:4633–4640 (2019).

[107] Li J., Lu Y., Ye Q., Cinke M., Han J., Meyyappan M., Carbon Nanotube Sensors for Gas and Organic Vapor Detection, *Nano. Letters*, **3(7)**: 929-933 (2003).

[108] Hadipour N.L., Peyghan A.A., Soleymanabadi H., Teoretical Study on the Al-Doped ZnO Nanoclusters for CO Chemical Sensors, *J. Physic. Chem*, **119(11)**: 6398-6404 (2015).

[109] Ahmadi A., Hadipour N.L., Kamfiroozi M., Bagheri Z., Theoretical Study of Aluminum Nitride Nanotubes for Chemical Sensing of Formaldehyde, Sensors, *Actuators. B. Chem*, **161(1)**: 1025-1029 (2012).

[110] Beheshtian J., Peyghan A.A., Bagheri Z., Detection of Phosgene by Sc-Doped BN Nanotubes: A DFT Study, *Sensors. Actuators B. Chem.*, **171**: 846–852 (2012).

[111] Zhao T.H., Wang M.K., Hai G.J., Chu Y.M., Landen Inequalities for Gaussian Hypergeometric Function. Revista de la Real Academia de Ciencias Exactas, *Físicas y Naturales. Serie A. Matemáticas*, **116(1)**: 1-23 (2022).

[112] Nazeer M., Hussain F., Khan M.I., El-Zahar E.R., Chu Y.M., Malik M.Y., Theoretical Study of MHD Electro-Osmotically Flow of third-grade fluid in micro channel. *Applied Mathematics and Computation*, **420**: 126868 (2022).

[113] Zhao T.H., Khan M.I., Chu Y.M., Artificial Neural Networking (ANN) Analysis for Heat and Entropy Generation in Flow of Non- Newtonian Fluid Between Two Rotating Disks, Mathematical Methods in the Applied Sciences, 1–19 (2021).

[114] Zhao T.H., Wang M.K., Zhang W., Chu Y.M., Quadratic Transformation Inequalities for Gaussian Hypergeometric Function, *Journal of Inequalities and Applications*, **2018(1)**: 1-15 (2018).

[115] Zhao T., Wang M., Chu Y., On the Bounds of the Perimeter of an Ellipse,*Acta Mathematica Scientia*, **42(2)**: 491-501(2022).

[116] Zha T.H., Castillo, O., Jahanshahi H., Yusuf A., Alassafi M.O., Alsaadi F.E., Chu Y.M., A Fuzzy-Based Strategy to Suppress the Novel Coronavirus (2019-NCOV) Massive Outbreak, *Applied and Computational Mathematics*, **20(1)**:160-176 (2021).

[117] Iqbal M.A., Wang Y., Miah M.M., Osman M.S., Study on ate–Jimbo–Kashiwara–Miwa Equation with Conformable Derivative Dependent on Time Parameter to Find the Exact Dynamic Wave Solutions, *Fractal and Fractional*, **6(1)**: 4 (2021).

[118] Zhao T.H., He Z.Y., Chu Y.M., Sharp Bounds for the Weighted Hölder Mean of the Zero-Balanced Generalized Complete Elliptic Integrals, *Computational Methods and Function Theory*, **21(3)**: 413-426 (2021).

[119] Zhao T.H., Wang M.K., Chu Y.M., Concavity and Bounds Involving Generalized Elliptic Integral of the First Kind, *J. Math. Inequal.*, **15(2):** 701-724 (2021).

[120] Chu H.H., Zhao T.H., Chu Y.M., Sharp Bounds for the Toader Mean of order 3 in Terms of Arithmetic, Quadratic and Contraharmonic Means, *Mathematica Slovaca*, **70(5)**:1097-1112 (2020).

[121] Zhao T.H., He Z.Y., Chu Y.M., On Some Refinements for Inequalities Involving Zero-Balanced Hypergeometric Function, *AIMS Math*, **5(6)**: 6479-6495(2020).

[122] Zhao T.H., Wang M.K., Chu, Y.M., A Sharp Double Inequality Involving Generalized Complete Elliptic Integral of the First Kind, *AIMS Math*, **5(5)**: 4512-4528 (2020).

[123] Zhao T.H., Shi L., Chu Y.M., Convexity and Concavity of the Modified Bessel Functions of the First Kind with Respect to Hölder Neans. Revista de la Real Academia de Ciencias Exactas, Físicas y Naturales, *Serie A. Matemáticas*, **114(2)**: 1-14 (2020).

[124] Zhao T.H., Zhou B.C., Wang M.K., Chu Y.M., On Approximating the Quasi-Arithmetic Mean, *Journal of Inequalities and Applications*, **2019(1)**: 1-12 (2019).
[125] Chu,Y.M., Zhao T.H., Concavity of the Error Function with Respect to Hölder Means, *Math. Inequal. Appl.*, **19(2)**: 589-595 (2016).
[126] Zhao T.H., Shen Z.H., Chu Y.M., Sharp Power Mean Bounds for the Lemniscate Type Means, Revista de la Real Academia de Ciencias Exactas, Físicas y Naturales. Serie A. Matemáticas, **115(4)**: 1-16 (2021).
[127] Song Y.Q., Zhao T.H., Chu Y.M., Zhang X.H., Optimal Evaluation of a Toader-Type Mean by Power Mean, *Journal of Inequalities and Applications*, **2015(1)**: 1-12 (2015).
[128] Chu Y.M., Zhao T.H., Convexity and Concavity of the Complete Elliptic Integrals with Respect to Lehmer Mean, *Journal of Inequalities and Applications*, **2015(1)**: 1-6 (2015).
[129] Zhao T.H., Yang Z.H., Chu Y.M., Monotonicity Properties of a Function Involving the psi Function with Applications, *Journal of Inequalities and Applications*, **2015(1)**: 1-10 (2015).